

Likelihood and Deep Learning Analysis of the electron neutrino event sample at Intermediate Water Cherenkov Detector (IWCD) of the Hyper-Kamiokande experiment

T. Mondal ^{a,*} N. W. Prouse ^b P. de Perio ^c M. Hartz ^d and D. Bose ^e on behalf of the Hyper-Kamiokande Collaboration

^aDepartment of Physics, Indian Institute of Technology Kharagpur
Kharagpur, West Bengal 721302, India

^bImperial College London, Department of Physics, London, United Kingdom

^cKavli Institute for the Physics and Mathematics of the Universe (WPI), The University of Tokyo Institutes for Advanced Study, University of Tokyo, Kashiwa, Chiba, Japan

^dTRIUMF, Vancouver, British Columbia, Canada

^eDepartment of Physics, Central University of Kashmir, Ganderbal,
Jammu & Kashmir 191131, India

E-mail: mtanima14@gmail.com

Hyper-Kamiokande (Hyper-K) is a next-generation long baseline neutrino experiment. One of its primary physics goals is to measure neutrino oscillation parameters precisely, including the Dirac CP violating phase. As conventional ν_μ beam generates from the J-PARC neutrino baseline contains only 1.5% of ν_e interaction of total, it is challenging to measure $\nu_e/\bar{\nu}_e$ scattering cross-section on nuclei. To reduce these systematic uncertainties, IWCD will be built to study neutrino interaction rates with higher precision. Simulated data comprise $\nu_e CC0\pi$ as the main signal with $NC\pi^0$ and $\nu_\mu CC$ are major background events. To reduce the backgrounds initially, a log-likelihood-based reconstruction algorithm to select candidate events was used. However, this method sometimes struggles to distinguish π^0 events properly from electron-like events. Thus, a Machine Learning-based framework has been developed and implemented to enhance the purity and efficiency of ν_e events.

42nd International Conference on High Energy Physics (ICHEP2024)
18-24 July 2024
Prague, Czech Republic

*Speaker

1. Introduction

Hyper-Kamiokande (Hyper-K) is a next-generation underground water Cherenkov detector, with a fiducial volume of eight times that of the existing Super-Kamiokande detector [1] and an upgraded neutrino beam power of ~ 1300 kW [2]. Its primary aim is to measure neutrino oscillation [3] by observing neutrinos from accelerator, atmospheric, solar, supernova and other astrophysical sources. One of the key physics goals of this long-baseline ($L = 295$ km) experiment is to investigate matter-antimatter asymmetry by measuring CP violation (CPV) in the neutrino sector [4].

A major challenge of this experiment lies in the precise measurement of electron neutrino cross-sections, which account for only 1.5% of those created by conventional muon neutrino (ν_μ) beam. To reduce these systematic uncertainties, an Intermediate Water Cherenkov detector (IWCD) [5] will be positioned about ~ 750 m downstream from the J-PARC neutrino source. The IWCD comprises an inner detector (ID) radius of 400 cm, and height of 300 cm, representing a fiducial volume of ~ 600 ton and equipped with ~ 500 high-resolution multi-PMT (mPMT) [2] modules, each consisting of an array of 19 smaller 8 cm diameter PMTs. This provides a granularity comparable to that of Hyper-K's far detector (FD). The detector volume of IWCD can move vertically within a 50 m tall pit, allowing the neutrino spectra to span $1^\circ - 4^\circ$ off-axis angle [2] to study neutrino interaction rate at different peak energies with high accuracy. With its new detector technologies, IWCD will be capable of measuring the percent level electron neutrino (anti) (ν_e or $\bar{\nu}_e$) contribution within ν_μ beam, as well as measuring cross-section ratios ($\sigma_{\nu_e}/\sigma_{\nu_\mu}$, $\sigma_{\bar{\nu}_e}/\sigma_{\bar{\nu}_\mu}$). This will significantly improve the CPV sensitivity by reducing the associated systematic uncertainties.

To achieve these goals, advanced event reconstruction algorithms are essential for accurate particle identification (PID) and for the measurement of ν_e cross-sections. This work explores the ν_e event selection using both the traditional event reconstruction algorithm (fiTQun) and the advanced Machine Learning (ML) tool. The analysis presented here demonstrates how the ML techniques improve event selection, signal purity, and its efficiency, surpassing fiTQun.

2. IWCD Event reconstruction and Particle identification with fiTQun

Inside a water Cherenkov detector (WCD), when charged particles like electrons or muons travel faster than the speed of light in water, they polarize the surrounding atoms, causing the emission of cone-shaped blue light known as Cherenkov light. PMTs surrounding the detector volume record the number of these photons and their arrival time [6]. By analysing the spatial and temporal distribution of the signal received by the hit PMTs, the event reconstruction algorithm determines, in part, particle type, momentum, energy and interaction location. Electrons produce broader, fuzzier Cherenkov rings due to multiple scattering and electromagnetic showering while they travel through the medium. Meanwhile, heavier muons undergo less scattering and typically produce a sharper Cherenkov ring.

2.1 IWCD event selection with fiTQun

FiTQun [6] is a likelihood-based event reconstruction algorithm used to reconstruct high-energy events inside WCD. It estimates the likelihood of the observed Cherenkov light pattern based on different particle hypotheses Γ (such as e^- , μ^- , or π^0) and reconstructs kinematic variables, including position, direction, and momentum, using the PMT's hit time and charge information. The likelihood ratios for different particle hypotheses are used to classify each event. For a given

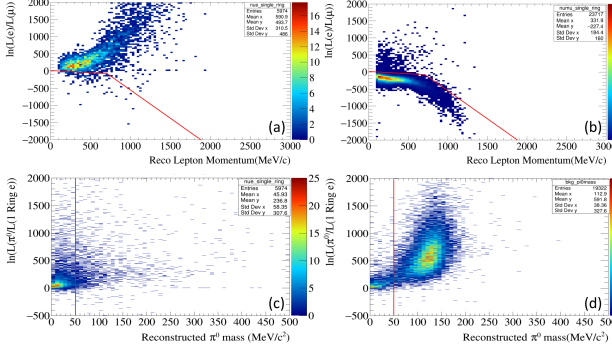


Figure 1: 2D histograms depicting the distribution of $\nu_e CC 0\pi$ signal in panels (a) and (c) and background events $\nu_\mu CC$ in panel (b), and $NC\pi^0$ in panel (d). In each panel the log-likelihood ratios are shown with respect to either the reconstructed lepton momentum or the reconstructed π^0 mass.

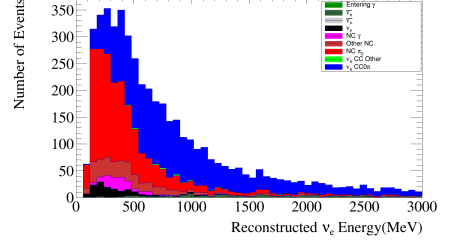


Figure 2: Interaction modes in the final selected ν_e events as a function reconstructed electron neutrino energy using fitQun reconstruction algorithm.

event hypothesis (e.g., electron or muon), the likelihood function L can be maximized by varying kinematic parameters θ . The likelihood function is defined as follows [7, 8]:

$$L(\Gamma, \theta) = \prod_j^{unhit} P_j(unhit|\Gamma, \theta) \prod_i^{hit} \{1 - P_i(unhit|\Gamma, \theta)\} \times f_q(q_i|\Gamma, \theta) f_t(t_i|\Gamma, \theta) \quad (1)$$

In this analysis, $P_j(unhit|\Gamma, \theta)$ is the probability that a PMT does not register a hit for a given hypothesis (Γ, θ) , while $P_i(hit|\Gamma, \theta)$ is the probability of a PMT being hit. The reconstructed variables are defined by the kinematic parameters that maximize this likelihood. In the analysis, these parameters are D_{wall} (distance from the vertex to the nearest detector wall), T_{wall} (distance to the nearest wall in the particle's direction), kinetic energy, momentum and mass. They are crucial for distinguishing signal from background events. To accurately measure electron neutrino cross-sections, we have selected a sample enriched with electron neutrino interactions, where $\nu_e CC 0\pi$ is the main signal and $NC\pi^0$, and $\nu_\mu CC$ are backgrounds. Events are simulated at an off-axis angle of 2.39° with a total exposure of 1×10^{17} protons on target (POT) in FHC (Forward Horn Current) mode, where the beam is mainly composed of ν_μ . This analysis uses NEUT as the neutrino interaction generator, WCSim to simulate the detector response and fitQun for the event reconstruction.

Result — To significantly reduce background contamination and improve the PID accuracy, we define a fiducial volume (FV) with $D_{wall} > 100$ cm and $T_{wall} > 100$ cm and select events with a reconstructed momentum of at least 100 MeV/c. Besides requiring single-ring events, additional cuts are applied to exclude events producing decay electrons and muons which penetrate the outer detector. To select ν_e candidates, relative log-likelihood cuts are used to remove $\nu_\mu CC$ and $NC\pi^0$ events (see Figure 1). The Figure of Merit ($FOM = \frac{S}{\sqrt{S+B}}$) is used to optimize the cut lines. In Figure 1, the red lines represent the boundary of the cuts, below which events are classified as background. Figure 2 shows the final selected events as a function of the reconstructed neutrino energy after applying all cuts and Table 1 summarizes these results. As one can see in Figure 2, $\nu_\mu CC$ are heavily suppressed, and the dominant remaining background in the final data sample is NC events. In the case of boosted π^0 decays, the two γ s can either overlap or one of them can carry

most of the energy causing fitQun to reconstruct the π^0 as a single ring electron-like event. This analysis achieved a $\nu_e CC0\pi$ purity of 51.1% with an efficiency of 69.5% (see Table 1). FitQun's detailed and computationally complex likelihood allows it to process at most 1 event per minute. Improvements in accuracy require more complex likelihoods with fewer simplifying assumptions, further increasing the computational demand beyond a realistically feasible level.

3. Machine Learning (ML) for Electron Neutrino Event Selection

ML techniques, particularly Convolutional Neural Networks (CNNs) [9], offer significant potential for extracting information from complex images. These can contribute to high-accuracy particle identification [10]. They also allow for reconstructing kinetic information (momentum, direction and interaction vertex) and for distinguishing between single and multi-ring events. In our analysis, we utilized a ResNet-18 architecture [11], which is an 18-layer CNN, within the WatChMaL [12] framework, to classify and reconstruct events inside both the IWCD and the Hyper-K far detector [13].

This configuration offers faster training times compared to other deep neural networks. Initially, we trained our Resnet-18 model for 20 epochs on four-particle classes (e^- , μ^- , γ , π^0) with 3 million of events each. The kinetic energy of each particle is uniformly distributed up to 1 GeV above the Cherenkov threshold. Figure 3 compares the performance of fitQun and ResNet-18 models from the ROC (Receiver Operating Characteristic) curve for γ background rejection against electron signal efficiency. The ResNet model, with an AUC (Area Under the Curve) of 0.7183, significantly outperforms fitQun (AUC of 0.5418) in separating electron signals from γ backgrounds.

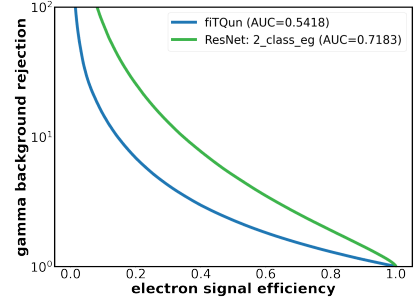


Figure 3: Comparison between fitQun and ML performance in γ /electron separation.

Motivated by the performance of the ML framework in distinguishing particle gun events (e^- , μ^- , γ , and π^0), we applied it to select ν_e events from a simulated beam profile. This IWCD simulated dataset contains single-ring CCQE ($\nu_e CC0\pi$, $\nu_\mu CC$), NC (NC γ , NC π^0), and other events such as more complex CC events with pions and/or multiple other outgoing particles in the final state with uniform energies ranging from 0 to 1.2 GeV. This test dataset is used for ML model evaluation and results in four softmax probabilities $P(e)$, $P(\mu)$, $P(\gamma)$ and $P(\pi^0)$ corresponding to e^- , μ^- , γ , and π^0 respectively. Then we further generated 2D histograms plotting $P(\mu)$ and $P(\pi^0)$ softmax probability against reconstructed momentum for $\nu_e CC0\pi$, $\nu_\mu CC$ and $NC\pi^0$ (Figure 4). Based on the distribution of signal and background in the histograms, we manually tuned three discriminators across $P(\mu)$, $P(\pi^0)$, and $P(e)$ to improve both the purity and efficiency. After applying all these ML cuts sequentially along with the basic FV and kinematic variable cuts (as defined for the fitQun-based analysis), the sample's purity improved to 61.5%, with an increased efficiency of 78.2% (Table 1). Figure 5, showcases that by suppressing $\nu_\mu CC$, all ML cuts significantly reduce the number of NC events, which dominated in the fitQun scenario previously, and hence, in this case, $\nu_e CC0\pi$ signal dominates over all other backgrounds (see Table 1).

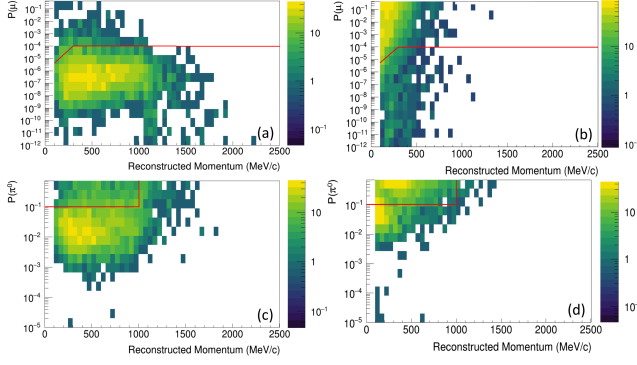


Figure 4: 2D histograms depicting the distribution of $\nu_e CC 0\pi$ signal in panels (a) and (c), background events $\nu_\mu CC$ in panel (b), and $NC\pi^0$ in panel (d). In each panel the softmax probability is shown with respect to the reconstructed lepton momentum.

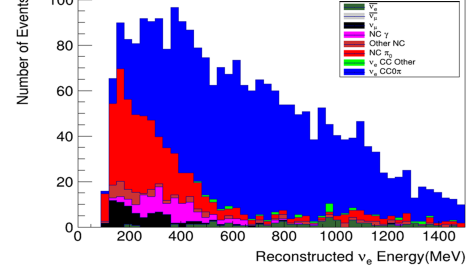


Figure 5: Interaction modes in the final selected ν_e events using ResNet-18 model classification.

Table 1: Comparison of purity and efficiency between fitQun and ML methods for the selected ν_e sample separated by true interaction modes.

Cuts Applied	$\nu_e CC 0\pi$	$\nu_\mu CC$	Total NC	$NC\pi^0$	$NC\gamma$	$\nu_e CC$ other	$\bar{\nu}_e$	$\bar{\nu}_\mu$	Purity	Efficiency
fitQun	2535	144	2100	1544	121	24	157	1	51.1%	69.5%
ML	2856	77	1342	627	93	79	288	0	61.5%	78.2%
ML/fitQun	1.13	0.54	0.64	0.41	0.77	3.29	1.83	0	—	—

4. Conclusion

This work evaluated the performance of ML techniques for electron neutrino event selection in IWCD compared to fitQun. While the latter achieved a purity of 51.1% with an efficiency of 69.5%, ML softmax cuts improved purity to 61.5% with an increased efficiency of 78.2%. With further development of more complex and automated ML cuts, we expected even more improvements beyond what is reported here.

Acknowledgements

T. Mondal acknowledges the support of the Prime Minister's Research Fellowship (PMRF). T. Mondal thanks the Mitacs Globalink Research Award (GRA) for supporting her research visit to TRIUMF, Canada.

References

- [1] K Abe, C Bronner, Y Haga, Y Hayato, M Ikeda, K Iyogi, J Kameda, Y Kato, Y Kishimoto, Ll Marti, et al. Atmospheric neutrino oscillation analysis with external constraints in superkamiokande i-iv. *Physical Review D*, 97(7):072001, 2018.
- [2] Hyper-Kamiokande Proto-Collaboration, :, K. Abe, Ke. Abe, H. Aihara, A. Aimi, R. Akutsu, C. Andreopoulos, I. Anghel, et al. Hyper-kamiokande design report, 2018.

- [3] Y Ashie, J Hosaka, K Ishihara, Y Itow, J Kameda, Y Koshio, A Minamino, C Mitsuda, M Miura, S Moriyama, et al. Evidence for an oscillatory signature in atmospheric neutrino oscillations. *Physical review letters*, 93(10):101801, 2004.
- [4] Hiroshi Nunokawa, Stephen Parke, and José W.F. Valle. Cp violation and neutrino oscillations. *Progress in Particle and Nuclear Physics*, 60(2):338–402, Apr 2008.
- [5] Mark Scott. An intermediate water cherenkov detector at j-parc. In *Proceedings of the 10th International Workshop on Neutrino-Nucleus Interactions in Few-GeV Region (NuInt15)*, page 010039, 2016.
- [6] RB Patterson, EM Laird, Y Liu, PD Meyers, I Stancu, and HA Tanaka. The extended-track event reconstruction for miniboone. *Nuclear Instruments and Methods in Physics Research Section A: Accelerators, Spectrometers, Detectors and Associated Equipment*, 608(1):206–224, 2009.
- [7] Andrew D Missert, T2K Collaboration, et al. Improving the t2k oscillation analysis with fitqun: a new maximum-likelihood event reconstruction for super-kamiokande. In *Journal of Physics: Conference Series*, volume 888, page 012066. IOP Publishing, 2017.
- [8] M Jiang, K Abe, C Bronner, Y Hayato, M Ikeda, K Iyogi, J Kameda, Y Kato, Y Kishimoto, L I Marti, et al. Atmospheric neutrino oscillation analysis with improved event reconstruction in super-kamiokande iv. *Progress of Theoretical and Experimental Physics*, 2019(5):053F01, 2019.
- [9] Yann LeCun, Yoshua Bengio, and Geoffrey Hinton. Deep learning. *nature*, 521(7553):436–444, 2015.
- [10] Nick Prouse. Advances in simulation and reconstruction for Hyper-Kamiokande. In *Proceedings of 40th International Conference on High Energy physics — PoS(ICHEP2020)*, volume 390, page 919, 2021.
- [11] Kaiming He, Xiangyu Zhang, Shaoqing Ren, and Jian Sun. Deep residual learning for image recognition. In *Proceedings of the IEEE conference on computer vision and pattern recognition*, pages 770–778, 2016.
- [12] WatChMaL. Watchmal: Github repository. <https://github.com/WatChMaL/WatChMaL>. GitHub repository.
- [13] Nicholas Prouse, Patrick de Perio, and Wojciech Fedorko. Machine learning techniques to enhance event reconstruction in water cherenkov detectors. In *Physical Sciences Forum*, volume 8, page 63. MDPI, 2023.